Ecological Indicators 165 (2024) 112200

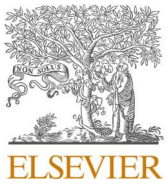

Contents lists available at ScienceDirect

Ecological Indicators

journal homepage: www.elsevier.com/locate/ecolind

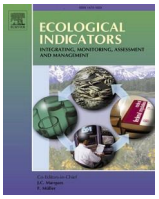

Original Articles

Predicting the dissolved natural organic matter (DNOM) concentration and the specific ultraviolet absorption (sUVa) index in a browning central European stream

Ståle Haaland [a,b,*], Josef Hejzlar [c], Bjørnar Eikebrokk [d], Geir Orderud [e], Ma. Cristina Paule-Mercado [c], Petr Porcal [c], Jiří Sláma [c,f], Rolf David Vogt [g]

[a] Norwegian Institute of Bioeconomy Research, NIBIO, 1431 Ås, Norway
[b] Norwegian University of Life Sciences, 1433 Ås, Norway
[c] Biology Centre of the Czech Academy of Sciences, 370 05 České Budějovice, Czech Republic
[d] Drikkevannskonsult, 7047 Trondheim, Norway
[e] Oslo Metropolitan University, 0130 Oslo, Norway
[f] Prague University of Economics and Business, 377 01 Jindrichuv Hradec, Czech Republic
[g] Norwegian Institute for Water Research, 0579 Oslo, Norway

ARTICLE INFO

Keywords:
Specific ultraviolet absorbance (sUVa) index
Dissolved natural organic matter (DNOM)
Regression models
Climate Change
Drinking water
Czech Republic

ABSTRACT

Over the past four decades, an increase in Dissolved Natural Organic Matter (DNOM) and colour, commonly referred to as *browning,* has been noted in numerous watercourses in the northern hemisphere. Understanding the fluctuations in DNOM quality is a prerequisite for gaining insights into the biogeochemical processes governing DNOM fluxes. Such knowledge is also pivotal for water treatment plants to effectively tailor their strategies for removing DNOM from raw water. The specific ultraviolet absorbance (sUVa) index has been a widely applied measurement for assessing DNOM quality. The sUVa index is the UV absorbance (OD_{254}) of water normalized for DNOM concentration. We have used a long-term dataset spanning from 2007 to 2022, taken from the Malše River in South Bohemia, to model DNOM and the sUVa index. We have applied regression models with a process-oriented perspective and have also considered the influence of climate change. Both DNOM and the sUVa index is positively related to temperature, runoff and *p*H, and negatively related to ionic strength over the studied period. Two distinct model approaches were employed, both explaining about 40% of the variation in sUVa over the studied period. Based on a moderate IPCC monthly climate scenario, simulations indicate that both DNOM and the sUVa index averages remain fairly stable, with a slight increase in winter season minima projected towards the year 2099. A slight decline in summer season maxima is simulated for DNOM, while the sUVa summer maximum remain stable. These findings suggest a robust resilience in both DNOM and the sUVa index against anticipated changes in temperature and runoff for the Malše River in South Bohemia.

1. Introduction

Allochthonously produced Dissolved Natural Organic Matter (DNOM) undergoes mineralization or becomes sequestered in catchment soils, with only a small fraction reaching surface waters (e.g., Kalbitz et al., 2000; Schmidt et al., 2011; Kaiser & Kalbitz, 2012). However, in recent decades, a widespread browning phenomenon, known as *brownification*, has been observed in freshwater bodies across the northern hemisphere, a phenomenon primarily attributed to an increased influx of allochthonous DNOM into surface waters (Finstad et al., 2016; Monteith et al., 2007; Vogt et al., 2023). Common indicators for DNOM levels include Ultraviolet (UV) absorbance at λ_{254} nm (OD_{254}) and the concentration of dissolved organic carbon (DOC). The wavelength at λ_{254} nm corresponds to a specific UV-C wavelength generated by the low-pressure mercury lamps (Rubin, 2010). The specific ultraviolet absorbance (sUVa) index, which normalizes the UV absorbance of DNOM for the concentration of DOC, is often utilized to assess the quality of DNOM. The OD_{254} is strongly affected by ferric iron concentrations, particularly due to overlaps between the DNOM and iron UV light absorbance (e.g., Turner and Miles, 1957; Poulin et al., 2014;

* Corresponding author at: Norwegian Institute of Bioeconomy Research, NIBIO, 1431 Ås, Norway.
E-mail address: staale.haaland@nibio.no (S. Haaland).

https://doi.org/10.1016/j.ecolind.2024.112200
Received 22 March 2024; Received in revised form 14 May 2024; Accepted 29 May 2024
Available online 1 June 2024

Haaland et al., 2018; Solberg, 2022). The sUVa index was by Weishaar et al. (2003) not found to accurately describe the reactivity of DNOM from different sources, however more recently it has been demonstrated by using a somewhat different approach that the sUVa index can be used as a simple and versatile tool for distinguishing between aromatic allochthonous and humic DNOM, from less aromatic autochthonous and more fulvic DNOM, as well as anthropogenic dissolved organic matter (Vogt et al., 2023). DNOM have an impact on surface raw waters and aquatic ecosystems and DNOM with different sUVa index value have also been reported to have had different impacts on mixotrophic algal densities in both epi- and hypolimnion in DNOM rich lakes (Rohrlack, 2023; Eikebrokk et al., 2018; Thrane et al., 2014; Algesten et al., 2004; Kirk, 1976). Moreover, the sUVa index is employed by drinking water treatment plants as a metric for DNOM treatability and the potential for disinfection byproduct formation (Fabris et al., 2008; Jaffé et al., 2008; Eikebrokk et al., 2004; Kitis et al., 2001; El-Shafy & Grünwald, 2000; Hua et al., 2015).

The rise in DNOM concentrations over the recent decades, especially pronounced from the early 1980 s to the early 2000 s, has been linked to decreased acid rain deposition (Tipping & Hurley, 1988; Forsberg & Petersen, 1990; Monteith et al., 2007; Haaland et al. 2007, 2010; de Wit et al., 2021). Humic substances (HS) comprise a major brown to black coloured portion of DNOM, and the solubility and mobility of HS in dilute solutions increases with increasing *p*H, decreasing ionic strength, and also the type ions present (e.g., de Wit, 1992; Yang et al., 2021). A decrease in the ionic strength in dilute solutions results in a higher zeta potential (a measure of electrostatic colloidal electrostatic or charge interaction) and a thicker diffuse double layer (DDL; i.e. increasing the Debye length), which will result in increased repulsion between colloids, reduced flocculation, and less coagulation (e.g., Larsen, 2024). The DDL thickness is also affected by cation valence, and according to the Hardy Schulze rule the coagulating power of an electrolyte at a similar ionic strength increases with the valency of the active ions (e.g., Derjaguin & Landau, 1993; Verwey & Overbeek, 1948). It is however somewhat comprehensive and expensive to calculate the ionic strength since it requires molar concentrations and hence chemical analysis of all the major ions. The conductivity is the sum of products of all ion activities (a) with their specific conductivities (Λ) (i.e., $Conductivity = \Sigma\ (a \cdot \Lambda)$). Since the limiting molar conductivities do not differ that much (50 to 160 μS cm^2 mol^{-1}), the conductivity is often linearly and strongly correlated to the ionic strength. Although there is a notable exception for H^+ (350 μS cm^2 mol^{-1}), its influence is negligible when *p*H is high (i.e., *p*H above 6; Golterman & Clymo, 1969). The measured conductivity, which is an easy parameter to measure (also *in situ*) with high accuracy and precision, has therefore often been used as a proxy for the ionic strength in modelling approaches in this context (e.g., Onsager, 1968; Golterman & Clymo, 1969). Humic acids (HA) and fulvic acids (FA) are major constituents of HS. The more coloured HA fraction is (operationally) defined as being soluble in water at neutral and alkaline *p*H. Both fractions will gain increased thickness of the DDL and thus higher solubility when the ionic strength is lowered in dilute solutions, while an increase in *p*H will also increase the solubility of HA (i.e. Yang et al., 2021; de Wit, 1992; Kipton et al., 1992). An increase in *p*H is expected to increase OD_{254} and, consequently, the sUVa index value. While *p*H from this might not be vital for models predicting DNOM developments if H^+ is included in the ionic strength calculation, it remains important for light absorbance models and, consequently, in a modelling approach for the sUVa index.

Another explanatory driver influencing DNOM dynamics, beyond those linked to DNOM solubility due to the previous long-term changes in acid rain deposition, is climate change. Concentrations of DNOM and UV absorbance in surface waters exhibit significant seasonal fluctuations and interannual variations, driven by climate parameters such as temperature and runoff (Finstad et al., 2016; de Wit et al., 2016; Svensson et al., 2008; Futter et al., 2007; Hejzlar et al., 2003). In addition to the long-term decline in acid rain (Monteith et al., 2007; de Wit et al., 2007), continuing trends in climate parameters are thus recognized as important explanatory drivers for the trends in DNOM and UV absorbance (de Wit et al., 2023; Haaland et al., 2023).

Temperature increases, particularly during spring and fall, extend the growing season, impacting catchment primary production (*greening*) and the microbial degradation of soil organic matter (i.e. Finstad et al., 2016). Changes in precipitation amount and intensity influence drought and flood frequencies, thereby altering drainage patterns (i.e. Haaland et al., 2010). During floods, shallow subsurface lateral soil water flow flushes the uppermost organic-rich soil layers. Notably, these upper soil layers exhibit high concentrations of humic-rich DNOM with high sUVa, and low *p*H, differing substantially from those found in deeper groundwater layers (Vogt et al., 2001). Thus, variations in solubility controlled by ionic strength and *p*H of a soil solution, coupled with differences in soil water flow paths, contribute to the observed temporal patterns in DNOM and UV absorbencies. During droughts and freezing soil temperatures limited drainage occurs from the upper DNOM-rich soils, instead runoff would mainly be generated by subsoil and groundwater discharge leading to lower sUVa index values in river water (i.e. Tipping et al., 2022). Drought conditions in mires and marshlands, on the other hand, can initiate the oxidation of sulphides to sulphates, increasing ionic strength and lowering *p*H in surface waters (Mosely et al., 2017; Massmann et al., 2003). Significant differences in sUVa index values may also arise from variations in catchment land use, and a forested sub-catchment often exhibits a higher sUVa index than a sub-catchment dominated by arable land (Vogt et al., 2023).

Models for UV absorbance and DOC concentrations serve as proxies for DNOM. Many of these rely on regression relationships and incorporate conceptually based parameters that influence DNOM abundance and solubility in soil solutions. Various models have been introduced to analyse temporal variations in DOC concentrations and light absorption (colour) in surface water systems, i.e., Monteith et al. (2023), Haaland et al. (2010), Hruška et al. (2009), Monteith et al. (2007), de Wit et al. (2007), Evans et al. (2006), and Hejzlar et al. (2003). The complex spatial heterogeneity of catchment properties and land use poses challenges for modelling. However, recognizing the drivers governing temporal changes in OD_{254} and DOC concentration in a watercourse is feasible through the utilization of high-resolution long-term monitoring data coupled with a robust process-oriented approach. However, there is a noticeable gap when it comes to models addressing changes in the quality of DNOM, particularly those reflecting alterations in the sUVa index. Since sUVa is determined by normalizing OD_{254} to the DOC concentration, modelling sUVa can be accomplished indirectly by simulating both OD_{254} and DOC. Alternatively, a direct modelling approach for sUVa is also feasible. In both cases, it is essential to interpret the simulation output with caution and within the considerations outlined above.

2. Material and methods

2.1. Study area

The study was conducted within the South Bohemian region of the Czech Republic, utilizing data from the Malše River. The Malše River is the main water source to the Římov reservoir, a drinking water supply for South Bohemia constructed in the 1970 s (Znachor, 2022). The reservoir spans a 13 km stretch of the Malše River (Fig. 1) and is the principal raw water source for the Plav drinking water treatment plant (Orderud et al., 2023), providing tap water to approximately 450,000 customers. The water chemistry of the Malše River has been monitored regularly since the late 1960 s, and the Římov reservoir has been integrated into the Czech long-term ecological research (LTER) network since 1997 (Church et al., 2022).

The dataset utilized for this study covers the period from 2007 to 2022 and comprises weekly average water chemistry data obtained from samples collected at the main river site in Pořešín, situated above the

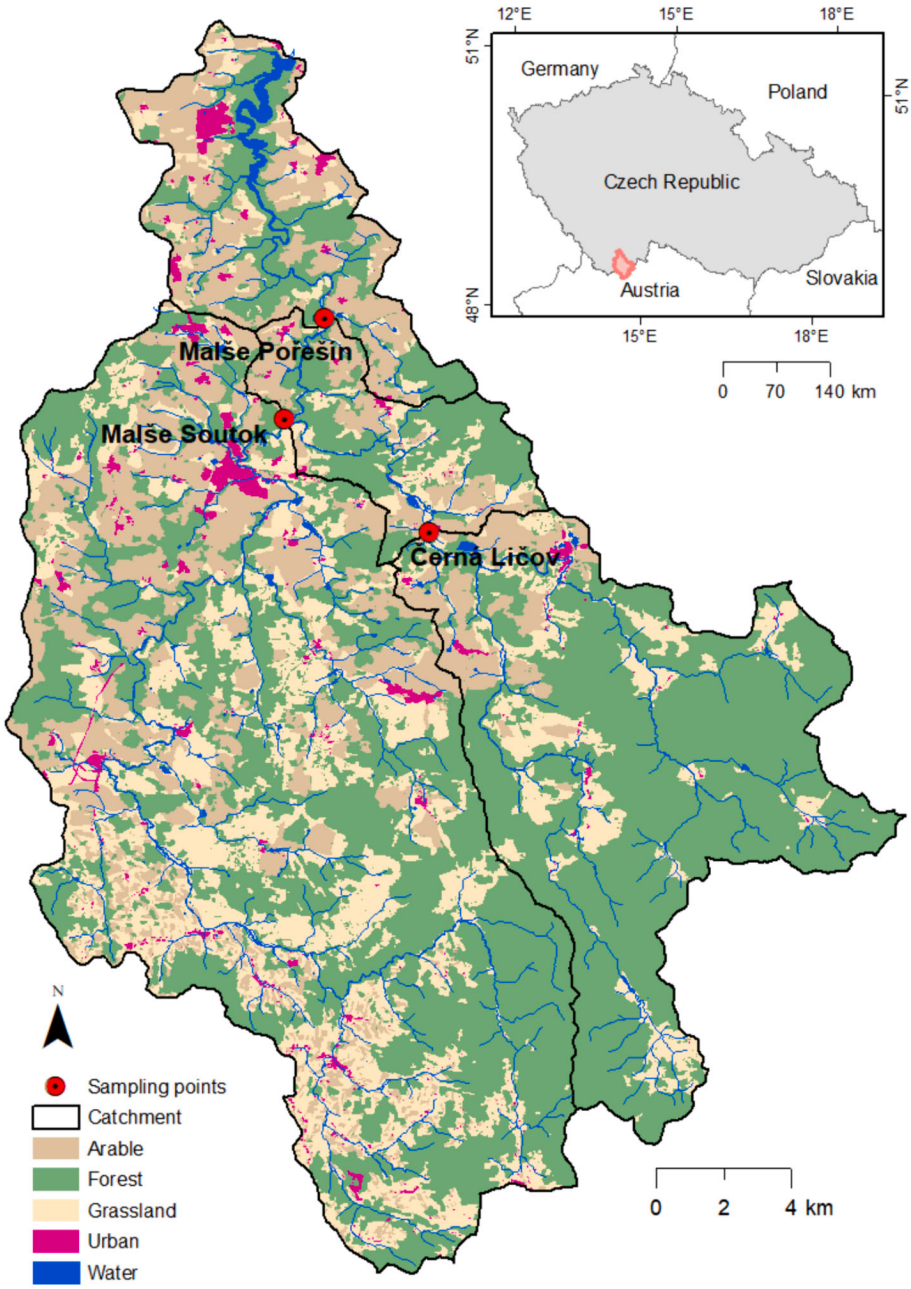

Fig. 1. The catchment of Římov reservoir, displaying land use patterns and the locations of sampling sites, within the South Bohemian region of the Czech Republic. Data was collected from the profile Malše Pořešín. Two major sub-catchments, Černá Ličov and Malše Soutok, contribute about 93% of the water draining to Malše Pořešín. Sampling sites also have measurements of temperature and runoff. See also https://porca.shinyapps.io/ Rimov_map_II/ for climate information.

reservoir inlet (Malše Pořešín, 48.7886422 N, 14.5168044E; Fig. 1). The total catchment area above Malše Pořešín encompasses 437 km^2, predominantly comprising 51 % forest, 46 % agricultural areas, 2 % urban areas, and 1 % surface water (Hejzlar et al., 2023).

DOC concentrations at Malše Pořešín have earlier been modelled in detail by Hejzlar et al. (2003). Since the mid-1980 s, there has been a positive increasing trend in the DOC concentration at Malše Pořešín, leading to a *brownification* in the Římov reservoir (Znachor et al., 2018). This rise has primarily been attributed to the decline in acid deposition (Hejzlar et al., 2003). Currently, the acid emissions in Europe are levelling off (Schöpp et al., 2003; Grennfelt et al., 2020). Instead, since the mid-1980 s, there has been an increasing trend in air temperature in the Czech Republic, including the Malše basin (Zahradníček et al., 2021). Climate change, with its effects on primary production (catchment *greening*), and alterations in hydrological regimes, is anticipated to further contribute to the *brownification* process in north European water sources (Crapart et al., 2023; de Wit et al., 2021; Finstad et al., 2016; Larsen et al., 2010; Haaland *et al.* 2007).

2.2. Chemical analyses

Water samples were analysed following ISO standard procedures at the Biology Centre CAS Institute of Hydrobiology in České Budějovice. Major anion concentrations were determined using ion chromatography. *p*H and conductivity were measured in the laboratory, while temperature and runoff were recorded on-site. Alkalinity was determined through Gran titration.

For the determination of Dissolved Organic Carbon (DOC) concentrations, 0.45 μm filtered samples were analysed using a total organic carbon analyser (Shimadzu TOC 5000A). UV absorbance at 254 nm

(OD_{254}) was measured in a 1 cm quartz cuvette using a double-beam UV/VIS spectrophotometer (Shimadzu UV-2700). The sUVa index was computed by normalizing UV absorbance to DOC concentrations (cm^{-1} at 254 nm / mg C L^{-1}). Data statistics are presented in Table 1.

2.3. Regression models

Regression analysis has been used in predicting the development of DNOM concentration and the sUVa index. The regression model set-up is similar to the ones used by Haaland et al., (2010). The structure is simple, transparent, and not overparameterized. There are several potential drivers for OD_{254}, DOC, and hence also the sUVa index. To be able to identify the most important ones, the response parameters were recognized using Principal Component Analysis (PCA).

3. Results

The water quality measured at Malše Pořešín indicates a fairly high *p*H (6.6–7.9 with a calculated mean of 7.3; Table 1), and the water also has some buffer capacity (197–813 $\mu mol_c\ L^{-1}$ alkalinity). Concentrations of DNOM (2.6–14.1 mg C L^{-1}), the sUVa index value (0.021 to 0.050), and also the conductivity (76–201 $\mu S\ cm^{-1}$) indicates some variation in water quality, which is also expected and for example due to seasonal variations in climate and catchment activity (Vogt et al., 2023). The Principal Component Analysis (PCA) performed on the Malše Pořešín dataset is shown in Fig. 2. The deduced drivers for the OD_{254}, DOC, and sUVa as response parameters in the PCA, include *p*H, conductivity, and major inorganic anions, along with a variable representing the percentage of water originating from different sub-catchments (CL%). The primary principal components, PC1 and PC2, collectively explain 62 % of the variance within the dataset. Notably, along the PC1 axis, OD_{254}, DOC concentration, and the sUVa index value exhibit high loadings, suggesting a gradient indicative of DNOM mobility. Conversely, PC2 is associated with the impact of hydrological soil water flow paths, evidenced by substantial loadings of fluctuations in discharge (lnQ), along with strong gradients in *p*H and carbonate alkalinity. The latter signifies the gradients in the soil profile, with relative high acidity in the organic-rich top horizons and high *p*H and alkalinity in the groundwater.

PC1 reveals an inverse relationship between conductivity (Cond), reflecting the ionic strength (I) of the soil solutions, and the OD_{254}, DOC concentration, and the sUVa index. Furthermore, these parameters are positively related to soil temperature (Tsoil) and runoff (lnQ). The mechanistic influence of Cond, Tsoil, and lnQ as explanatory parameters on sUVa, as the response parameter, can be conceptually rationalized by their combined effects on DNOM solubility, the production of DNOM from primary production and the microbial degradation of soil organic matter, as well as changes in soil water flow-paths from the upper soil organic-rich layers abundant in DNOM (DOC and OD_{254}). This contrasts with deeper groundwater soil layers characterized by higher *p*H and carbonate alkalinity (Vogt et al., 1990).

Bicarbonate (HCO_3^-), sulphate (SO_4^{2-}), chloride (Cl^-), and nitrate (NO_3^-) emerge as significant anions with a negative correlation to DOC, OD_{254}, and the sUVa value along PC1. This correlation can be attributed to diverse temporal variations in the sources of runoff, such as the presence of HCO_3^- from groundwater, NO_3^- and SO_4^{2-} from agricultural activities and (more pronounced in the earlier stages) from acid rain, and also processes like the oxidation of sulphides in mires and marshlands during drought conditions (Mosely et al., 2017; Massmann et al., 2003).

Table 1
Weekly averages of major anions and water quality data for Malše Pořešín for the years 2007–2022. The water is characterized by a high *p*H and bicarbonate alkalinity. Mean *p*H value is determined based on the H^+ concentration.

Analysis	Unit	n	Mean	Minimum	Maximum
Alk	$\mu mol_e\ L^{-1}$	762	571	197	813
SO_4^{2-}	mg L^{-1}	762	13.7	8.4	19.6
NO_3^-	mg L^{-1}	762	1.3	0.5	2.8
Cl^-	mg L^{-1}	762	7.1	2.5	21.4
*p*H		762	7.3	6.6	7.9
Cond	$\mu S\ cm^{-1}$	762	130	76	201
DOC	mg C L^{-1}	762	5.7	2.6	14.8
OD_{254}	$cm^{-1} \cdot 100$	765	0.5221.5	8.6	58.3
sUVa	cm^{-1} / mg C L^{-1}	765	0.037	0.021	0.050

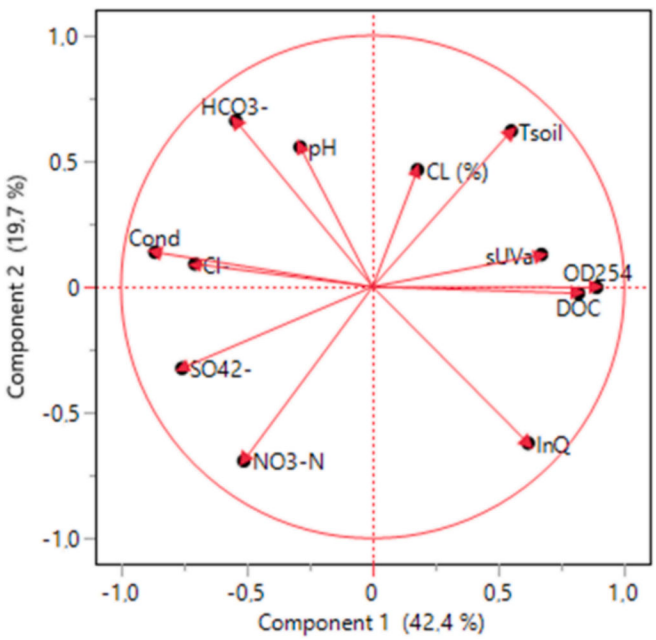

Fig. 2. Principal component analysis (PCA) of data for water chemistry in Malše River at Malše Pořešín. The data are weekly averaged measurements in water samples collected between 2007 and 2022. CL (%) is the percentage of water at Malše Pořešín originating from Černá Ličov, one of the two major sub-catchments draining to Malše Pořešín.

The correlations between the sUVa and its primary drivers, as deduced from the PCA – i.e., soil temperature, runoff, and conductivity, are shown in Fig. 3. Additionally, correlations with OD_{254} and DOC concentrations are included. While the relationship between the sUVa index and OD_{254} or DOC concentrations inherently intertwines, it remains valuable to highlight the relative roles of these proxies in measuring high and low sUVa index values.

Consistent with PCA findings, the sUVa index exhibits significant ($p < 0.01$) positive correlation with soil temperature, runoff, and a negative correlation with conductivity (Fig. 3). The sUVa index demonstrates a stronger association with OD_{254} ($r^2 = 0.40$) than with DOC concentrations ($R^2 = 0.16$). Notably, since runoff from the organic-rich topsoil is only possible when catchment soils are water-saturated and not frozen, the sUVa index attains its highest values during the wet summer and early autumn seasons.

The incorporation of conductivity data to model DNOM concentrations has been a common practice in various models (e.g., Monteith et al., 2007; Haaland et al., 2023). However, the solubility of DNOM is also somewhat dependent on *p*H (Yang et al., 2021). At Malše Pořešín, the *p*H ranges between 6.6–7.9, indicating a relatively high *p*H level. Notably, the *p*H tends to be lower in the upper organic rich soils, which contribute significantly to river flow during periods of high lnQ (Vogt et al., 1990). Consequently, a relatively weak but anticipated negative relationship along PC1 exists between *p*H and both OD_{254} and DOC, as well as the sUVa index. Given the distinct impact of pH on HA compared to FA fractions, it becomes intriguing to explore the incorporation of both *p*H and conductivity in a regression model for the sUVa index.

Temporal fluctuations in anionic composition can also be linked to

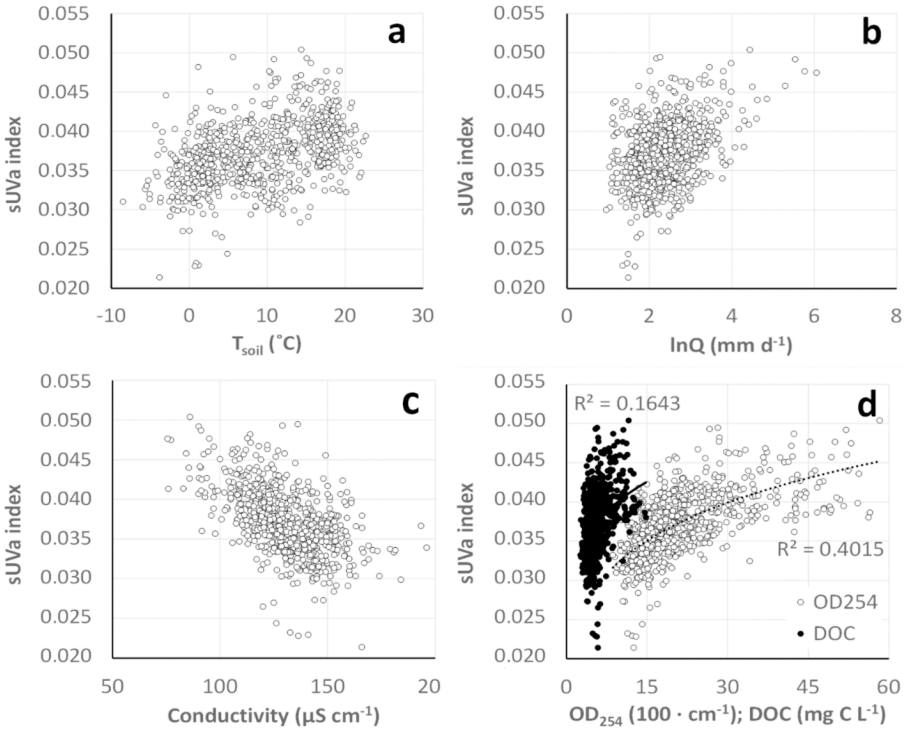

Fig. 3. The sUVa index plotted against key inferred drivers, i.e., soil temperature, runoff, and conductivity measured at Malše Pořešín from 2007 to 2022. Panel d showcases the non-linear correlation between the sUVa index and OD_{254}, as well as DOC concentrations.

variations in runoff from distinct sub-catchments. The two primary sub-catchments draining into Malše Pořešín are Černá Ličov and Malše Soutok (Fig. 1). The correlation between conductivity, the sUVa index, and the sum of major anions ($\Sigma(SO_4^{2-}, NO_3^-, Cl^-, HCO_3^-)$) measured at Malše Pořešín and the its two main (93 %) sub-catchments is illustrated in Fig. 4. Significantly lower conductivity is measured in the more forested Černá Ličov (Fig. 4a). As anticipated, in line with the study by Vogt et al. (2023), the sUVa index value is higher in the more dilute water from the more forested Černá Ličov compared to Malše Soutok (Fig. 4b). According to the PCA (Fig. 2), both the CL% and sUVa exhibit slight positive loadings along both PC1 and PC2. However, the positive correlation is very weak ($r^2 = 0.01$), probably attributed to a seemingly small temporal variation in differences between runoff amounts from Černá Ličov and Malše Soutok (Fig. 4c).

Temperature, runoff, conductivity, and *p*H were selected as explanatory parameters in the regression models based on the above deduction. The monitoring data for these model parameters at Malše Pořešín from 2007 to 2022 are presented in Fig. 5. For an indirect sUVa modelling approach using a model for OD_{254} normalized for a model for DOC concentration, we employed the following regression set-up for the OD_{254}:

$$OD_{254} = K_1 + k_1 \cdot (Q_{ln}^{a1} \cdot T_{soil}^{b1}) \cdot (pH^{c1}) \cdot (Conductivity^{d1}) \quad (1)$$

The regression model structure set-up chosen is comparable to regression model setup has been previously adopted by Haaland et al., (2010). Likewise for the DOC concentration:

$$DOC = K_2 + k_2 \cdot (Q_{ln}^{a2} \cdot T_{soil}^{b2}) \cdot (pH^{c2}) \cdot (Conductivity^{d2}) \quad (2)$$

The parameters K and k serve as adjusting factors for values and units of measurement. Weekly averaged measurements were utilized, employing a straightforward mean of runoff amounts (Q, mm d^{-1}) over the sampling period, as opposed to incorporating a lag in runoff, with the only modification being a simple adjustment to mitigate the impact of runoff peaks:

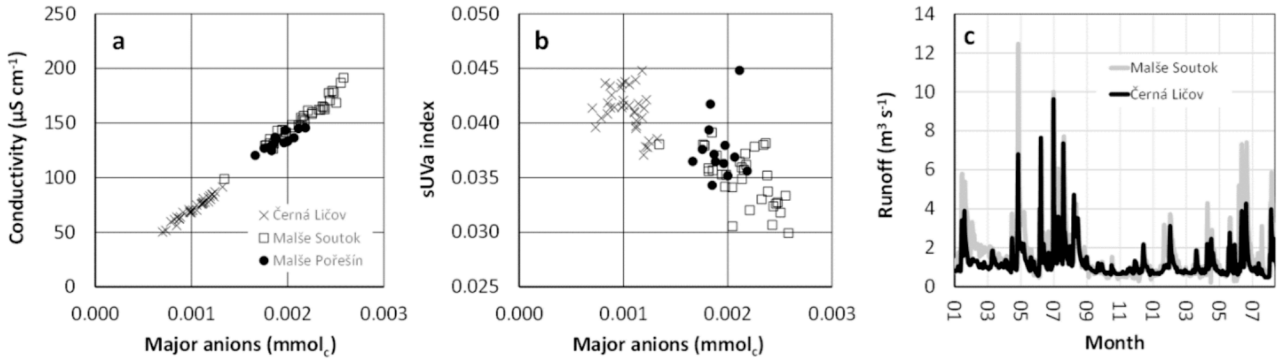

Fig. 4. Differences between water characteristics from the two primary sub-catchments for Malše Pořešín. Panel a illustrates the variances in conductivity, while panel b shows fluctuations in the sUVa plotted against major anions in water samples collected at Černá Ličov (crosses), Malše Soutok (open squares), and Malše Pořešín (filled circles). Panel c displays the runoff from Černá Ličov (black line) and Malše Soutok (grey line). The dataset comprises samples collected every third week throughout the years 2021 and 2022.

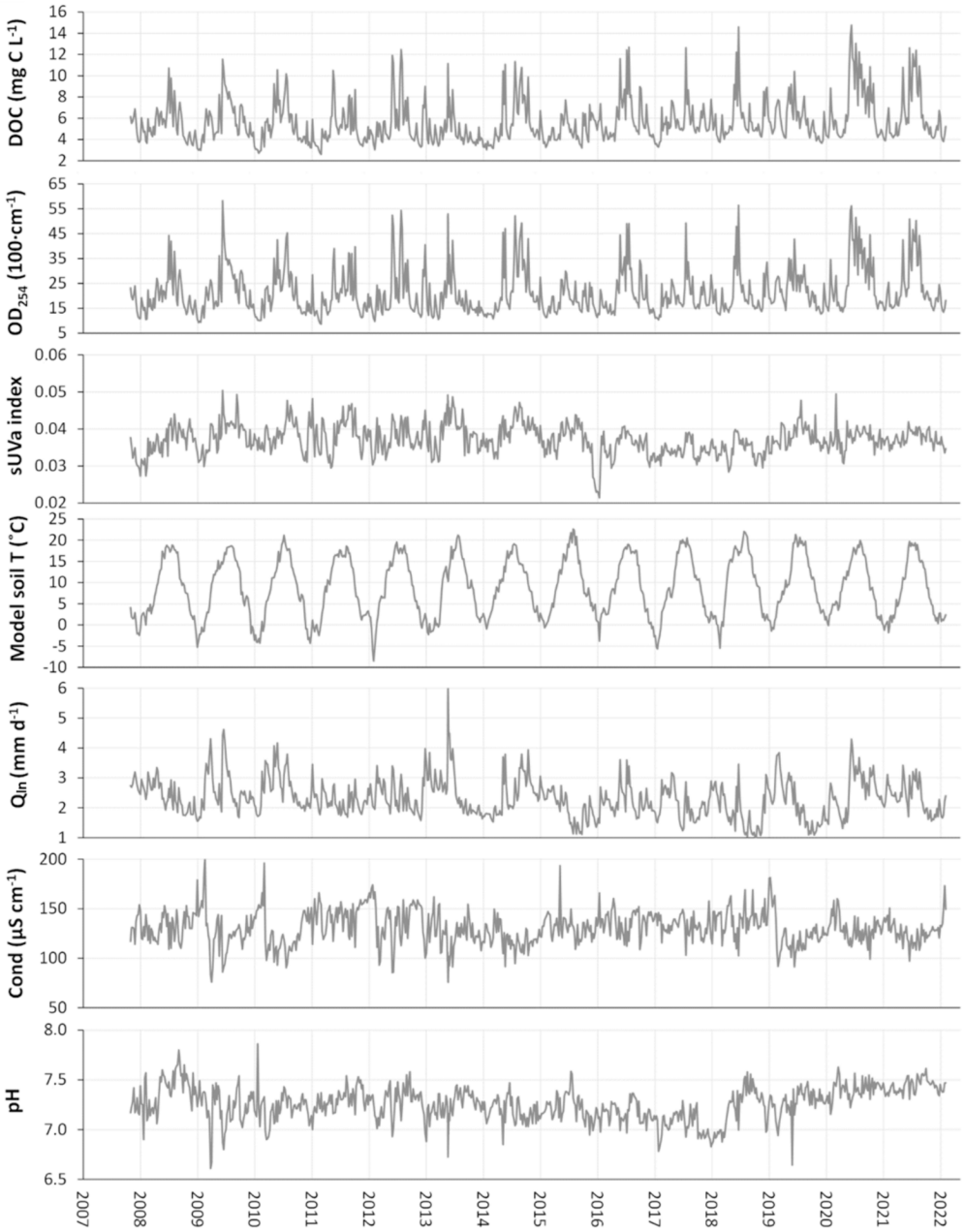

Fig. 5. Weakly averaged data from 2007 to 2022 of DOC concentration, OD_{254} values, conductivity and *p*H in water sampled at Malše Pořešín, along with calculated sUVa index level, modelled soil temperature (T_{soil}; *Eq.* *(4)*, and runoff (Q_{ln}; *Eq.* *(3)*.

$$Q_{ln} = ln(Q) + y \tag{3}$$

Here y is a positive integer keeping the Q_{ln} expression > 0. This is done because ***Eq.*** ***(1)*** and ***Eq.*** ***(2)*** uses exponents. y is set to 3.

The soil temperature (T_{soil}) is derived from measured air temperature and an empirical soil temperature model for the catchment soils:

$$T_{soil} = [0.53 \cdot (Tair_{0-2} + k_T) + 0.45 \cdot (Tair_{3-23} + k_T)] + z \tag{4}$$

$Tair_{0\text{-}2}$ is the mean air temperature for today and the two previous days, and $Tair_{3\text{-}23}$ the mean air temperature measured between the previous 3–23 days. k_T is an empirical catchment specific constant and is for the Malše Pořešín catchment set to −2.0 °C (based on Hejzlar et al., 2003, 2023). z is a positive integer set to 9 in order to keep the soil temperature T_{soil} expression positive by reasons as described for Q_{ln} above. From this the sUVa index can be calculated using sUVa = ***Eq.*** ***(1)*** · ***Eq.*** ***(2)*** $^{-1}$.

The temporal variation in OD_{254} and DOC at a given site often exhibits a robust linear correlation (Shi et al., 2022). This pattern is also evident in the analysed dataset, where the linear regression coefficient (R^2) was 0.94. Consequently, the slope of the regression line is frequently employed in a straightforward transfer calculation to estimate DOC concentration from optical OD_{254} measurements (Shi et al., 2022). However, the quotient of OD_{254} and DOC concentration, i.e., the sUVa index, is not a constant due to temporal fluctuations in aromaticity resulting from temporal variations in the sources of DNOM and its solubility. Hence, we have also conducted direct modelling of the sUVa index using a regression model set-up similar to the ones used for ***Eq.*** ***(1)*** and ***Eq.*** ***(2)***:

$$sUVa = K_3 + k_3 \cdot (Q_{ln}^{a3} \cdot T_{soil}^{b3}) \cdot (pH^{c3}) \cdot (Conductivity^{d3}) \tag{5}$$

The parameterization of the models was carried out utilizing the least sum of squares option in the Solver application provided in

Microsoft Excel. The data input used for fitting the model comprised odd years within the dataset, i.e., 2007, 2009, and so forth, up to 2021. The best-fit parameters obtained from odd years were compared with a best-fit parameterization performed using data input from all years (i.e., 2007, 2008, 2009 … 2022). Both approaches yielded similar results, as the simulations based on models parameterized using the two different sets of data showed strong correlations (R^2 ranging from 0.975 to 0.994; Fig. 6).

The results for calibration for constants and coefficients in ***Eq. (1)***, ***Eq. (2)***, and ***Eq. (5)*** are presented in Table 2. Approximately 71 % of the variations in weekly averaged UV absorbance measurements at Malše Pořešín between 2007–2022 are explained by ***Eq. (1)***. Similarly, ***Eq. (2)*** explains about 62 % of the variations in the DOC concentration (Fig. 6). The direct approach sUVa regression model (***Eq. (5)***) accounts for about 41 % of the variation within the dataset (Fig. 6). The indirect estimate for sUVa (i.e., ***Eq. (1)*** · ***Eq. (2)*** $^{-1}$) was not expected to have a similarly high R^2 since it involves the quotient of two modelled parameters. Nevertheless, due to the good simulation abilities for both OD_{254} via ***Eq. (1)*** and DOC concentration via ***Eq. (2)***, the indirect sUVa model explained about 40 % of the sUVa index variation.

The modelled OD_{254} and DOC concentration using ***Eq. (1)*** and ***Eq. (2)***, respectively, are shown in Fig. 7. The indirect and direct modelled values for sUVa (depicted by orange lines) are shown in Fig. 8a and b, respectively. While the seasonal fluctuations, characterized by higher index values during summer and lower values during the winter season, appear to be well-modelled, there are instances where certain high and low peaks in the sUVa index are not accurately captured (Fig. 8). Residual distribution plots are shown in Fig. 9.

As the *p*H coefficient in ***Eq. (2)*** is close to zero (Table 2), the inclusion of pH in the DOC model does not significantly enhance the explanatory power of the model. However, the *p*H coefficients are positive for both OD_{254} and the sUVa index. This could be attributed, in part, to the enhanced solubility of the less soluble and more UV-absorbing HA fractions of DNOM with an increasing *p*H compared to the FA fraction (Yang et al., 2021). Consequently, an increased *p*H, along with a lowered ionic strength in the upper soil layers, might also contribute to an increase in the sUVa index.

Table 2
Model constants and coefficients for regression models for OD_{254} (*Eq.* (1)), DOC (*Eq.* (2)) and the sUVa index (Eq. (5)). The parameterization was conducted using the Solver application in Microsoft Excel incorporating all data within the dataset (see text).

Model	Parameter	K	k	Q_{ln}	T_{soil}	Cond	*p*H
Eq. (1)	OD_{254}	7.6	11	0.95	0.85	−0.79	0.40
Eq. (2)	DOC	2.8	0.52	1.1	0.88	−0.32	−0.09
Eq. (5)	sUVa	0.025	0.032	0.16	0.23	−1.0	1.6

4. Discussion

Both the indirect and direct sUVa index models are indicating that sUVa is positively related to temperature, runoff and *p*H and negatively related to conductivity at Malše Pořešín (see ***Eq. (5)***). Still, low and high sUVa index values are found when UV absorbance (i.e., DNOM) is ditto low and high (Fig. 2). The lowest sUVa values occur during low flow winter and early spring (Figs. 6 and 7), while the highest are found during the wet summer and early autumn. The baseflow runoff is mainly constituted by groundwater, characterized by high *p*H and conductivity, and low content of DNOM, while the high runoff comprises more water from the topsoil layers, typically having low *p*H and conductivity, and

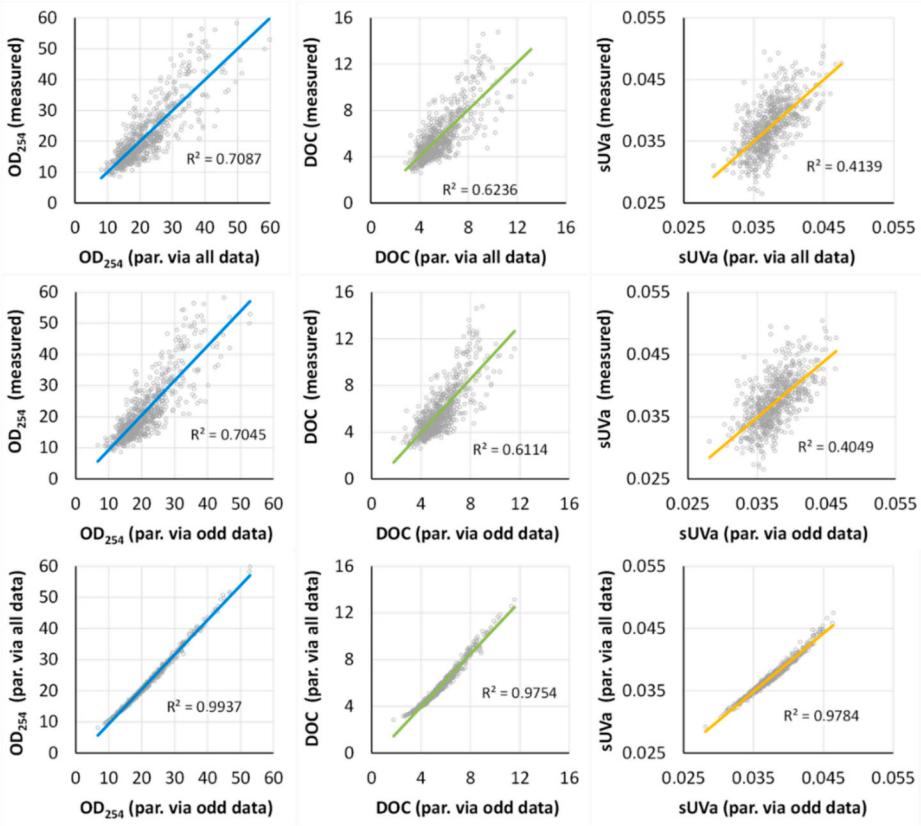

Fig. 6. Comparison of model performance between those parameterized (par.) using data from odd years only compared to models parameterized using all years of the 2007–2022 dataset. The two methods exhibit very similar performance. Linear regressions between measured data and the simulated values by different models are also shown. The models explain approximately 70–71% (OD_{254}; *Eq.* (1)), 61–62% (DOC concentration; *Eq.* (2)), and 40–41% (sUVa index; *Eq.* (5)) of the variation in the measured values.

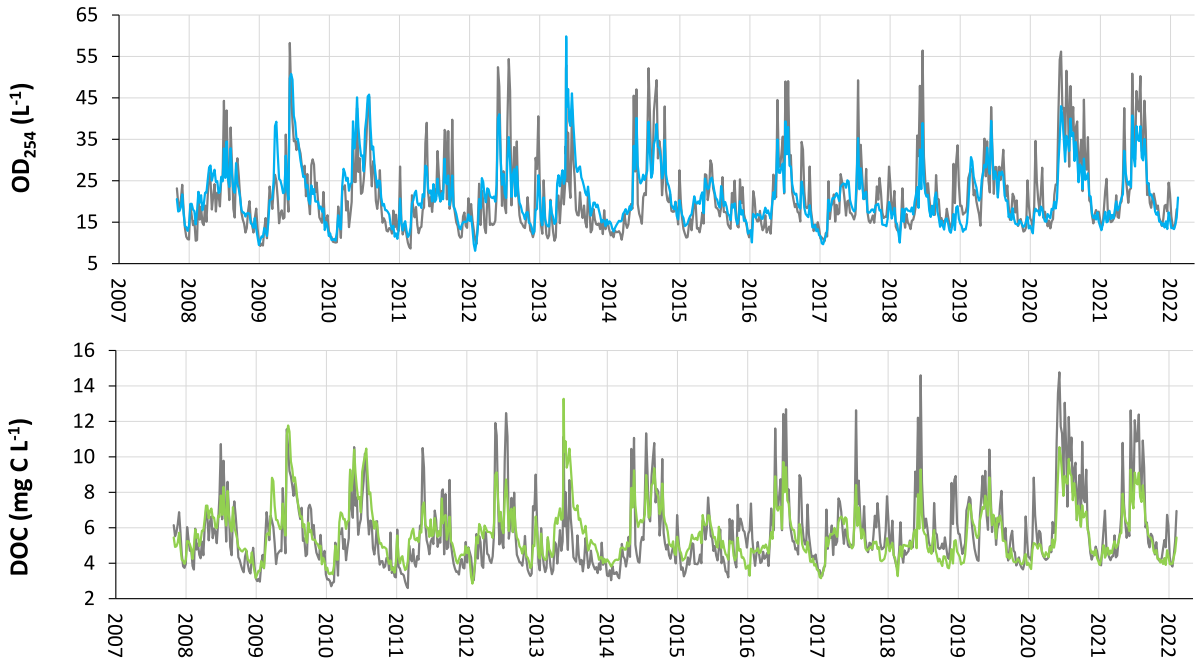

Fig. 7. Model performance for *Eq. (1)* (OD_{254}; blue line) and *Eq. (2)* (DOC concentration; green line) using data from water sampled at Malše Pořešín. Measured data are weekly averaged measurements between 2007–2022 (grey lines). The models explain approximately 71% (OD_{254}) and 62% (DOC concentration) of the measured variations. (For interpretation of the references to colour in this figure legend, the reader is referred to the web version of this article.)

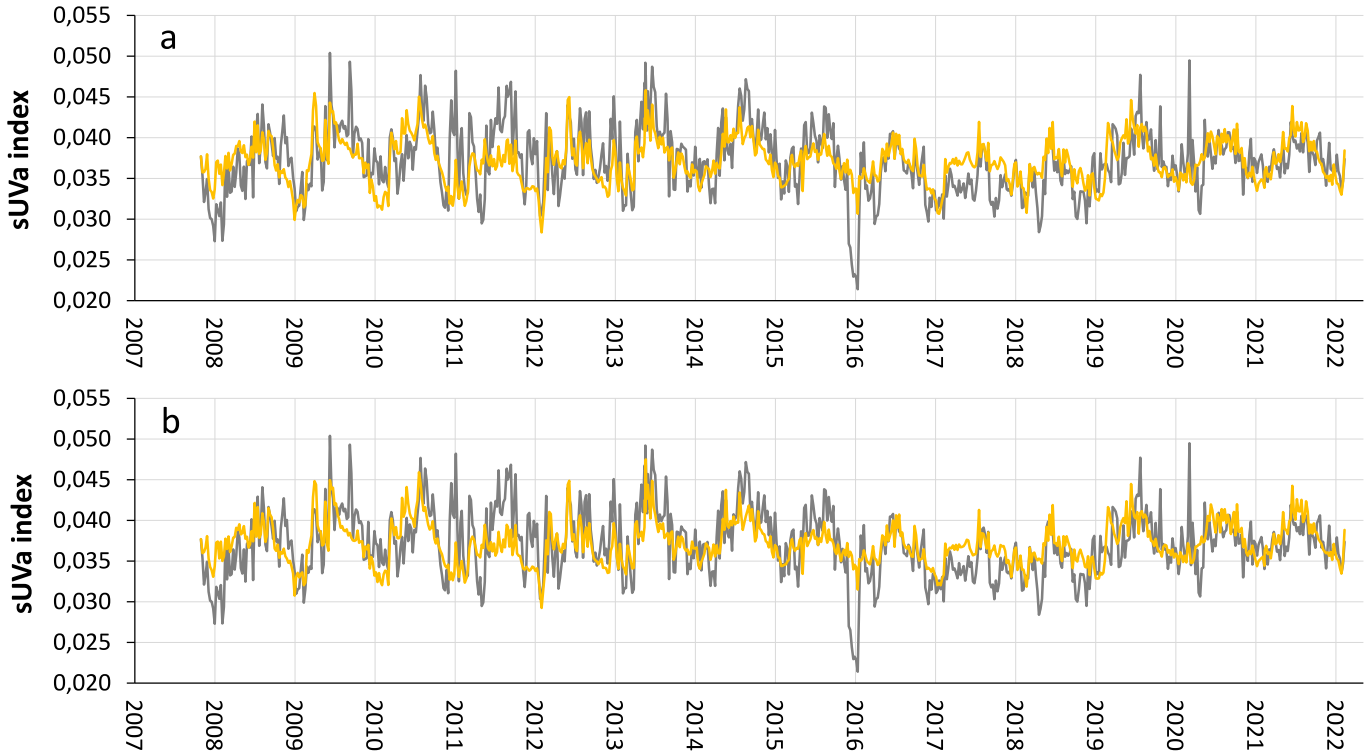

Fig. 8. Performance of the sUVa model (orange lines) calculated using *Eq. (1)*. *Eq. (2)* $^{-1}$ (a) and *Eq. (5)* (b) with data from water sampled at Malše Pořešín. The measured data consists of weekly averaged measurements from 2007 to 2022 (grey lines). The models explain approximately 40% (*Eq. (1)* · *Eq. (2)* $^{-1}$) and 41% (*Eq. (5)*) of the observed variation in the sUVa index values. Similar to OD_{254} and DOC concentration the sUVa index value tends to peak during summer and early autumn, while reaching its lowest levels during winter and early spring. (For interpretation of the references to colour in this figure legend, the reader is referred to the web version of this article.)

high content of DNOM. Fluctuations in soil water flow paths thus explain the seasonal variation in DNOM, but not the sUVa. The *p*H in groundwater is high while it is low in the topsoil. Based on the effects of the *p*H on the solubility of HA and FA, one would imply that the sUVa in the groundwater and topsoil be high and low, respectively – which is not the case. Still, the models do indicate that sUVa is positively related to *p*H.

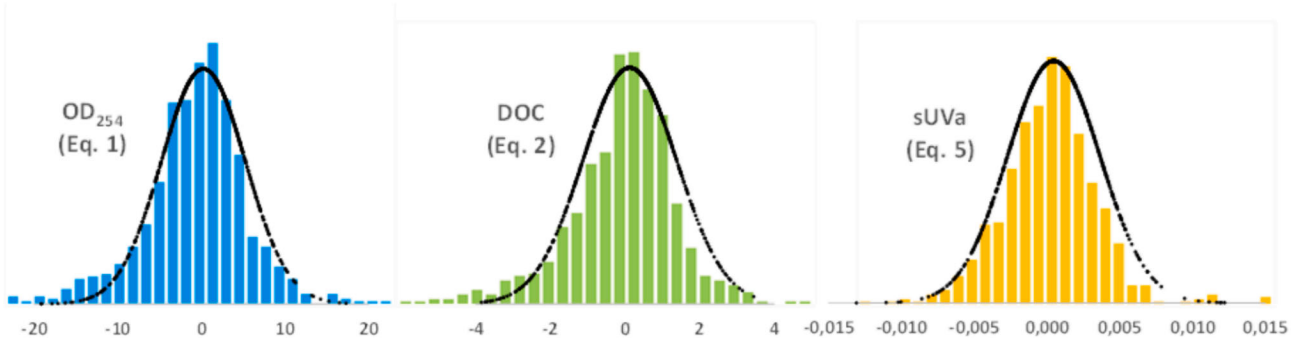

Fig. 9. Histograms showing the model residual distribution for water data samples at Malše Pořešín (2007–2022) using *Eq. (1)* (OD_{254}; blue line), *Eq. (2)* (DOC concentration; green line), and *Eq. (5)* (sUVa index; orange line). The residuals are following a normal distribution. The superimposed Bell curves are generated using the residual data. (For interpretation of the references to colour in this figure legend, the reader is referred to the web version of this article.)

This illustrates the antagonistic roles of the different governing processes, such as hydrology and solubility, on the sUVa. There is thus the need to include all the explanatory variables in the model. Since the sUVa index has an impact on aquatic ecosystems and is also used by drinking water treatment plants in assessing DNOM reactivity and treatability (Eikebrokk et al., 2004), understanding the potential impacts of climate change on the sUVa index is of significant importance.

Czechia is experiencing an accelerated water cycle, marked by higher temperatures and more precipitation (Vargas Godoy et al., 2024). Less snow and earlier snowmelt with an increase in runoff during winter and consequently less runoff in spring has also been found when comparing data from the previous reference period (1961–1990) to the present (1991–2020) (Vargas Godoy et al., 2024). Anticipating future changes in runoff for catchments facing concurrent temperature and precipitation increases poses a considerable challenge (e.g., Fallah et al., 2020; Zaitchik et al., 2023). However, projections for Czechia indicate that, with the predicted rise in temperatures and a corresponding surge in evapotranspiration, surpassing precipitation increments, a decrease in runoff and an escalation in drought occurrences are likely (Vargas Godoy et al., 2024).

For the studied area, climate predictions for the period 2070–2099, based on a moderate IPCC climate scenario (SSP2-4.5/CMIP6; Eyring et al., 2016; Meinshausen et al., 2020), suggest an average annual temperature increase of about 2.5–4 ºC, with most pronounced effects expected from July to September (Holtanová et al., 2022). Another research project, evaluating runoff trend from small, forested catchments in Czechia (the GEOMON network), used the Aladin-Climate/CZ regional climate model with the IPCC SRES A1B scenario (somewhat comparable to the more recent IPCC RCP6.0 scenario) and the BROOK90 hydrological model. This study predicted an annual decline in runoff of around 35 %, with a notable decrease in summer and a slight increase in winter until 2071–2100, in comparison to the reference period of 1994–2011 (Lamačová et al., 2014).

By using climate data inputs based on moderate climate predictions, which include higher temperatures and a hydrological regime characterized by drier springs and summers, we can generate moderate predictions for future UV absorbance, DOC concentration and sUVa index value at Malše Pořešín. The selected input data includes seasonal air temperature and runoff for 2070–2099, compared to present (year 2023) values, as shown in Table 3. Model simulations, using ***Eq. (1), Eq. (2)*** and ***Eq. (5)*** with input data reflecting gradual monthly changes in air temperature and runoff from present (year 2023) to year 2099, are shown in Fig. 10. Average weekly values for the last five years from the dataset sampled at Malše Pořešín (2007–2022) were used as selecting input data for conductivity and *p*H.

The regression models project a stable mean value for UV absorbance and DOC concentrations from present to 2099. This aligns with recent findings for DOC concentrations by Hejzlar et al. (2023). A slight decrease is anticipated during the summer season, attributed to the drier summers resulting in less drainage trough the more organic-rich topsoil (Hongve *et al.* 2003; Hagedorn et al., 2000; Table 3). Similarly, a slight elevation in the lowest concentrations during the winter season (Fig. 10) can be ascribed to increased runoff in the increasingly wetter winter season, coupled with low evapotranspiration leading to more substantial drainage through the organic-rich soil top horizon (Vargas Godoy et al., 2024; Table 3). The sUVa index value are also simulated to remain stable, with only a small increase in the winter season sUVa minima (from about 0.0335 to 0.0340). The simulations for the sUVa index value are very similar and exhibit not significantly differences ($p < 0{,}01$) when using either the indirect calculation via the quotient of OD_{254} and DOC concentration vs. the direct model for the sUVa index (***Eq. (5);*** Fig. 10c and d).

4.1. Early warning set-up for sUVa index values

The sUVa index can be accurately simulated if soil temperature, runoff, *p*H and conductivity are measured (***Eq. (5)***). All these parameters can be conveniently logged *in situ*. Predictive correlations also exist between low and high OD_{254} measurements and similarly low and high sUVa index values (Fig. 3d). Installing a simple single wavelength (SW) devise for *in situ* OD_{254} measurements is straightforward, robust and relatively inexpensive (Shi et al., 2022). Using a regression model set-up similar to that of OD_{254}, with weekly averaged measurements of OD_{254}, *p*H and conductivity sampled at Malše Pořešín between 2007–2022 as input parameters, and following the parametrization procedure as described above, the sUVa index is well explained ($R^2 = 0.47$). While the sUVa index and the OD_{254} measurements from Malše Pořešín are intercorrelated, *in situ* OD_{254} measurements from a well calibrated SW devise should provide accurate readings of OD_{254} similar to those obtained with a laboratory spectrophotometer (Table 1; Shi et al., 2022). A similar approach can be applied using more advanced multi-wavelength (MW) devise capable of differentiating ferric iron UV absorbance from

Table 3
Input data for monthly changes in air temperature and runoff for Malše Pořešín between present (year 2023) until year 2099. Data has been selected from model approaches using moderate climate scenarios (see text).

Month	J	F	M	A	M	J	J	A	S	O	N
Air temperature (C)	2.5	2.5	2.5	2.5	3.0	3.5	4.0	4.0	4.0	3.5	3.0
Runoff (Changes %)	0	−20	−40	−40	−40	−40	−40	−40	−20	−10	10

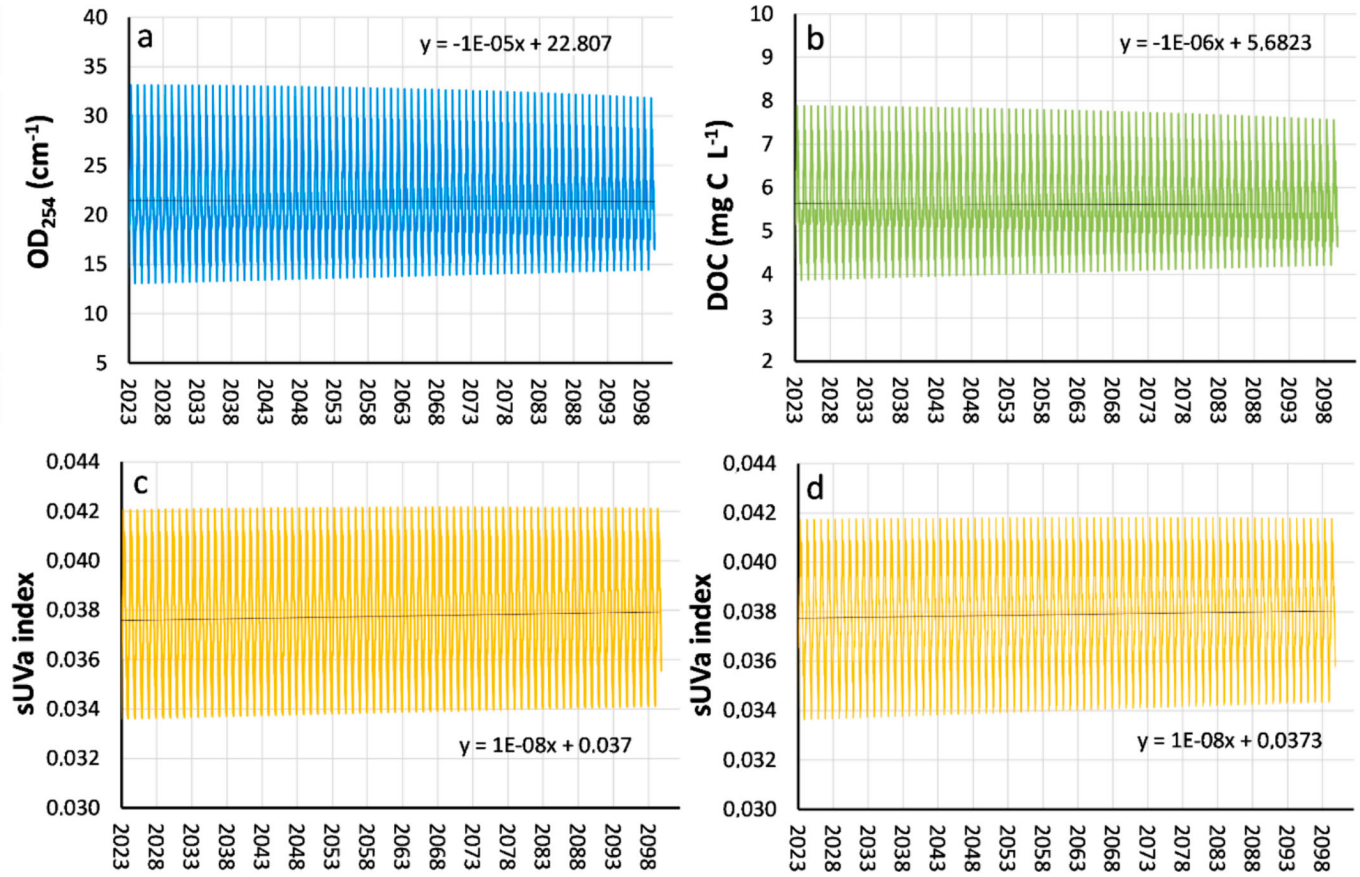

Fig. 10. Simulated future UV absorbance (OD_{254}), DOC concentrations, and sUVa index value. A moderate IPCC climate scenario until 2070–2099 has been used (Holtanová et al., 2022; see text). OD_{254} and DOC has been modelled using *Eq.* (1) and *Eq.* (2), respectively. The sUVa indexes have been modelled using the quotient between *Eq.* (1) and *Eq.* (2) (graph c), and the direct sUVa regression model *Eq.* (5) (graph d). Fairly stable maximum sUVa values during summer season and a slightly higher minima during winter season are simulated.

the DNOM contribution. Logging equipment should be placed strategically within a river network to provide early warnings, especially to entities such as drinking water treatment plants. A pilot in Rimov reservoir, run by the large Plav Drinking Water Treatment Plant should be considered. This would help gaining experience on location of and operating loggers as part of a larger system, providing data on economic and regulatory aspects in addition to technology. Also learning–knowledge processes in connection with running and using data from the system should be addressed. Results from the pilot should be discussed with other drinking water treatment plants in the area, focussing how the system can be adopted and adapted to fit other, and especially smaller plants.

5. Conclusion

The seasonal dynamic sUVa index in the Malše River, situated in the South Bohemian region of the Czech Republic, exhibits a distinctive pattern. The index attains its highest values during the summer and early autumn, while registering its lowest levels in winter and early spring. A robust predictive model for DNOM and the sUVa index has been established through simple multiple linear regressions, incorporating soil temperature, runoff, *p*H, and conductivity as explanatory parameters. Under a moderate climate scenario, projections suggest a slight decrease in DNOM for summer season maxima and a minor increase in winter season DNOM minima from present time onward until the year 2099. Furthermore, the sUVa index is anticipated to remain stable, with only a slight increase in winter season sUVa minima. Recognizing the significance of the sUVa index in influencing aquatic ecosystems and water treatment processes, the implementation of an early warning system, using strategically positioned loggers within the river network could prove beneficial.

Funding

The research was supported and funded by the TAČR KAPPA project Drinking WAter Readiness for the Future (DWARF) funded by the Norway Grants. No. 2020TO01000202.

CRediT authorship contribution statement

Ståle Haaland: Writing – original draft, Validation, Software, Methodology, Formal analysis, Data curation, Conceptualization. **Josef Hejzlar:** Writing – review & editing. **Bjørnar Eikebrokk:** Writing – review & editing. **Geir Orderud:** Writing – review & editing. **Ma. Cristina Paule-Mercado:** Writing – review & editing. **Petr Porcal:** Writing – review & editing, Project administration. **Jiří Sláma:** Writing – review & editing. **Rolf David Vogt:** Writing – review & editing, Conceptualization.

Declaration of competing interest

The authors declare that they have no known competing financial interests or personal relationships that could have appeared to influence the work reported in this paper.

Data availability

Data will be made available on request.

References

Algesten, G., Sobek, S., Bergström, A.K., Ågren, A., Tranvik, L.J., Jansson, M., 2004. Role of lakes for organic carbon cycling in the boreal zone. Global Change Biol. 10, 141–147. https://doi.org/10.1111/j.1365-2486.2003.00721.x.

Church MJ, Cloern JE, Evans-White M, Grebmeier JM, Hernández D, Laney CM, North G. Decadal Review of the Long-Term Ecological Research Program A Report of the 40 Year Review Committee. 2022. https://lternet.edu/wp-content/uploads/2022/06/nsf22200.pdf.

Crapart, C., Finstad, A.G., Hessen, D.O., Vogt, R.D., Andersen, T., 2023. Spatial predictors and temporal forecast of total organic carbon levels in boreal lakes. Sci. Total Environ. 870, 161676 https://doi.org/10.1016/j.scitotenv.2023.161676.

de Wit, J.C.M., 1992. Proton and Metal Ion Binding to Humic Substances. Wageningen Agricultural University, The Netherlands, 255 p. Doctoral thesis.

de Wit, H.A., Mulder, J., Hindar, A., Hole, L., 2007. Long-term increase in dissolved organic carbon in streamwaters in Norway is response to reduced acid deposition. Environ. Sci. Technol. 41, 7706–7713.

de Wit, H.A., Valinia, S., Weyhenmeyer, G.A., Futter, M.N., Kortelainen, P., Austnes, K., Hessen, D., Raike, A., Laudon, H., Vournenmaa, J., 2016. Current browning of surface waters will be further promoted by wetter climate. Environ. Sci. Technol. Lett. 3 (12), 430–435. https://doi.org/10.1021/acs.estlett.6b00396.

de Wit, H.A., Stoddard, J.L., Monteith, D.T., Sample, J.E., Austnes, K., Couture, S., Fölster, J., Higgins, S.N., Houle, D., Hruška, J., Krám, P., Kopáček, J., Paterson, A.M., Valinia, S., van Dam, H., Vuorenmaa, J., Evans, C., 2021. Cleaner air reveals growing influence of climate on dissolved organic carbon trends in northern headwaters. URL Environ. Res. Lett. 16, 104009. https://iopscience.iop.org/article/10.1088/1748-9326/ac2526.

de Wit, H.A., Garmo, Ø.A., Jackson-Blake, L., Clayer, F., Vogt, R.D., Kaste, Ø., Gundersen, C.B., Guerrerro, J.L., Hindar, A., 2023. Changing Water Chemistry in One Thousand Norwegian Lakes During Three Decades of Cleaner Air and Climate Change. Glob. Biogeochem. Cycles 37, e2022GB007509.

Derjaguin, B., Landau, L.D., 1993. Theory of the stability of strongly charged lyophobic sols and of the adhesion of strongly charged particles in solutions of electrolytes. Prog. Surf. Sci. 43 (1–4), 30–59. https://doi.org/10.1016/0079-6816(93)90013-L.

Eikebrokk B, Haaland S, Javris P, Riise G, Zahlsen K, Vogt, RD, Zahlsen K. 2018. NOMiNOR: Natural Organic Matter in drinking waters within the Nordic Region. Norwegian Water Report 2018; A231. ISBN 978-82-414-0406-1. https://va-kompetanse.no/butikk/a-231-nominor-natural-organic-matter-in-drinking-waters-within-the-nordic-region-kun-digital/.

Eikebrokk, B., Vogt, R.D., Liltved, H., 2004. NOM increase in Northern European source waters: Discussion of possible causes and impacts on coagulation/contact filtration processes. Wat. Sci. Technol. Water Supply 4 (4), 47–54. https://doi.org/10.2166/ws.2004.0060.

El-Shafy, M.A., Grünwald, A., 2000. THM formation in water supply in South Bohemia. Czech Republic. Water Research 34 (13), 3453–3459. https://doi.org/10.1016/S0043-1354(00)00078-6.

Evans, C.D., Chapman, P.J., Clark, J.M., Monteith, D.T., Cresser, M.S., 2006. Alternative explanations for rising dissolved organic carbon export from organic soils. Global Change Biol. 12, 2044–2053. https://doi.org/10.1111/j.1365-2486.2006.01241.x.

Eyring, V., Bony, S., Meehl, G.A., Senior, C.A., Stevens, B., Stouffer, R.J., Taylor, K.E., 2016. Overview of the Coupled Model Intercomparison Project Phase 6 (CMIP6) experimental design and organization. Geosci. Model Dev. 9, 1937–1958. https://doi.org/10.5194/gmd-9-1937-2016.

Fabris, R., Chow, C.W., Drikas, M., Eikebrokk, B., 2008. Comparison of NOM character in selected Australian and Norwegian drinking waters. Water Res. 42, 4188–4196. https://doi.org/10.1016/j.watres.2008.06.023.

Fallah, A., Sungmin, O., Orth, R., 2020. Climate-dependent propagation of precipitation uncertainty into the water cycle. Hydrol. Earth Syst. Sci. 24, 3725–3735. https://doi.org/10.5194/hess-24-3725-2020.

Finstad, A.G., Andersen, T., Larsen, S., Koji, T., Blumentrath, S., de Wit, H.A., Tømmervik, H., Hessen, D., 2016. From greening to browning: Catchment vegetation development and reduced S-deposition promote organic carbon load on decadal time scales in Nordic lakes. Sci. Rep. 6, 31944. https://doi.org/10.1038/srep31944.

Forsberg, C., Petersen, R.C., 1990. A darkening of Swedish lakes due to increased humus inputs during the last 15 years. Verh. Int. Verein. Limnol. 24, 289–292.

Futter, M.N., Butterfield, D., Cosby, B.J., Dillon, P.J., Wade, A.J., Whitehead, P.G., 2007. Modelling the mechanisms that control in-stream dissolved organic carbon dynamics in upland and forested catchments. Water Resour. Res. 43 (2), W02424. https://doi.org/10.1029/2006WR004960.

Golterman, H.L., Clymo, R.S., 1969. Methods for Chemical Analysis of Fresh Waters. Oxford, Edinburgh, published for the International Biological Programme by. Blackwell Scientific, 172p IBP handbook 8.ISBN 0632055405.

Grennfelt, P., Engleryd, A., Forsius, M., Hov, Ø., Rodhe, H., Cowling, E., 2020. Acid rain and air pollution: 50 years of pro-gress in environmental science and policy. Ambio 49 (4), 849–864. https://doi.org/10.1007/s13280-019-01244-4.

Haaland S, Riise G, Xiao Y-H. Iron vs NOM light absorbance - Could iron constrain the sUVa-index legitimacy? 2018; SIL-conference. Poster. https://doi.org/10.13140/RG.2.2.27156.40326.

Haaland, S., Riise, G., Hongve, D., Laudon, H., Vogt, R.D., 2010. Quantifying the drivers of increasing colored organic matter in boreal surface waters. Environ. Sci. Technol. 44 (8), 2975–2980. https://doi.org/10.1021/es903179j.

Haaland, S., Eikebrokk, B., Riise, G., Vogt, R.D., 2023. Browning of Scottish surface water sources exposed to climate change. PLOS Water 2 (9), e0000172. https://doi.org/10.1371/journal.pwat.0000172.

Haaland S, Riise G, Hongve D, Grøterud O, Blakar I. TOC concentrations in Norwegian lakes: The effect of sea-salts and anthropogenic acid components. SIL conference summer 2007. Verh. Int. Verein. Limnol. 30(9).

Hagedorn, F., Schleppi, P., Waldner, P., Fluhler, H., 2000. Export of dissolved organic carbon and nitrogen from gleysol dominated catchments—the significance of water flow paths. Biogeochemistry 50, 137–161. https://doi.org/10.1023/A:1006398105953.

Hejzlar, J., Dubrovský, M., Buchtele, J., Růžička, M., 2003. The apparent and potential effects of climate change on the inferred concentration of dissolved organic matter in a temperate stream (the Malse River, South Bohemia). Sci. Total Environ. 310 (1–3), 143–152. https://doi.org/10.1016/S0048-9697(02)00634-4.

Hejzlar J, Porcal P, Kopáček J, Jarošík J, Paule-Mercado Ma C. Forecast model of DOC in the inflow to the Římov water reservoir and in the withdrawal of water from the reservoir. Proc. Conf. Water Supply Biology 2023, February 9–10, 2023, Prague, Czech Republic, Říhová Ambrožová J, Petráková Kánská K (Eds)], Vodní zdroje EKOMONITOR spol. s r. o., Chrudim, ISBN 978-80-88238-26-3, pp. 45–50. (In Czech).

Holtanová, E., Belda, M., Halenka, T., 2022. Projected changes in mean annual cycle of temperature and precipitation over the Czech Republic: Comparison of CMIP5 and CMIP6. Front. Earth Sci. 10, 1018661 https://doi.org/10.3389/feart.2022.1018661.

Hruška, J., Krám, P., McDowell, W.H., Oulehle, F., 2009. Increased dissolved organic carbon (DOC) in Central European streams is driven by reductions in ionic strength rather than climate change or decreasing acidity. Environ. Sci. Technol. 43 (12), 4320–4326. https://doi.org/10.1021/es803645w.

Hua, G., Reckhow, D.A., Abusallout, I., 2015. Correlation between SUVA and DBP formation during chlorination and chloramination of NOM fractions from different sources. Chemosphere 130, 82–89. https://doi.org/10.1016/j.chemosphere.2015.03.039.

Jaffé, R., McKnight, D., Maie, N., Cory, R., McDowell, W.H., Campbell, J.L., 2008. Spatial and temporal variations in DOM composition in ecosystems: The importance of long-term monitoring of optical properties. J. Geophys. Res. 113, G04032 https://doi.org/10.1029/2008JG000683.

Kaiser, K., Kalbitz, K., 2012. Cycling downwards – dissolved organic matter in soils. Soil Biol. Biochem. 52, 29–32. https://doi.org/10.1016/j.soilbio.2012.04.002.

Kalbitz, K., Solinger, S., Park, J.H., Michalzik, B., Matzner, E., 2000. Controls on the dynamics of dissolved organic matter in soils: a review. Soil Sci. 165 (4), 277–304. https://doi.org/10.1097/00010694-200004000-00001.

Kipton, H., Powell, J., Raewyn, M.T., 1992. Solubility and fractionation of humic acid; effect of pH and ionic medium. Anal. Chim. Acta 267 (1), 47–54. https://doi.org/10.1016/0003-2670(92)85005-Q.

Kirk, J.T.O., 1976. Yellow substance (gelbstoff) and its contribution to the attenuation of photosynthetically active radiation in some inland and coastal south-eastern Australian waters. Aust J Mar Freshw Res. 27, 61–71. https://doi.org/10.1071/MF9760061.

Kitis, M., Karanfil, T., Kilduff, J.E., Wigton, A., 2001. The reactivity of natural organic matter to disinfection by-products formation and its relation to specific ultraviolet absorbance. Water Sci. Technol. 43, 9–16. https://doi.org/10.2166/wst.2001.0067.

Lamačová, A., Hruška, J., Krám, P., Stuchlík, E., Farda, A., Chuman, T., Fottová, T., 2014. Runoff trends analysis and future projections of hydrological patterns in small, forested catchments. Soil & Water Res. 9 (4), 169–181. https://doi.org/10.17221/110/2013-SWR.

Larsen, D., 2024. Physical Chemistry. LibreTexts. https://chem.libretexts.org/@go/page/182379.

Larsen, S., Andersen, T., Hessen, D.O., 2010. Climate change predicted to cause severe increase of organic carbon in lakes. Global Change Biol. 17 (2), 1186–1192. https://doi.org/10.1111/j.1365-2486.2010.02257.x.

Massmann, G., Tichomirowa, M., Merz, C., Pekdeger, A., 2003. Sulfide oxidation and sulfate reduction in a shallow groundwater system (Oderbruch Aquifer, Germany). J. Hydrol. 278 (1–4), 231–243. https://doi.org/10.1016/S0022-1694(03)00153-7.

Meinshausen, M., Nicholls, Z.R., Lewis, J., Gidden, M.J., Vogel, E., Freund, M., et al., 2020. The shared socio-economic pathway (SSP) greenhouse gas concentrations and their extensions to 2500. Geosci. Model. Dev. 13 (8), 3571–3605. https://doi.org/10.5194/gmd-13-3571-2020.

Monteith, D.T., Stoddard, J.L., Evans, C.D., de Wit, H.A., Forsius, M., Høgåsen, T., Wilander, A., Skjelkvåle, B.L., Jeffries, D.S., Vuorenmaa, J., Keller, B., Kopáček, J., Veselý, J., 2007. Dissolved organic carbon trends resulting from changes in atmospheric deposition chemistry. Nature 450, 537–541. https://doi.org/10.1038/nature06316.

Monteith, D.T., Henrys, P.A., Hruska, J., de Wit, H.A., Krám, P., Moldan, F., Posch, M., Raike, A., Stoddard, J.L., Shilland, E.M., Pereira, M.G., Evans, C.D., 2023. Long-term rise in riverine dissolved organic carbon concentration is predicted by electrolyte solubility theory. Sci. Adv. 9 (3), eade349 https://doi.org/10.1126/sciadv.ade3491.

Mosely, L.M., Biswas, T.K., Cook, F.J., Marschner, P., Palmer, D., Shand, P., Yuan, C., Fitzpatric, R.W., 2017. Prolonged recovery of acid sulfate soils with sulfuric materials following severe drought: causes and implications. Geoderma 308, 312–320. https://doi.org/10.1016/j.geoderma.2017.03.019.

Onsager, L., 1968. The motion of ions: Principles and concepts. Nobel Lecture. https://www.nobelprize.org/uploads/2018/06/onsager-lecture.pdf.

Orderud, G.I., Porcal, P., Eikebrokk, B., Sláma, J., Vogt, R.D., Hejzlar, J., Haaland, S., 2023. The technological development of drinking water treatment plants in the Czech Republic. Water Policy 25 (9), 889–907. https://doi.org/10.2166/wp.2023.102.

Poulin, B.A., Ryan, J.N., Aiken, G.R., 2014. Effects of iron on optical properties of dissolved organic matter. Environ Sci Technol 48 (17), 10098–10106.

Rohrlack, T., 2023. Can osmotrophy in Gonyostomum semen explain why lake browning drives an expansion of the alga in parts of Europe? Limnologica 101, 126097. https://doi.org/10.1016/j.limno.2023.126097.

Rubin, M.B., 2010. The development of the mercury lamp. Bull. Hist. Chem. 35 (2), 105–110.

Schmidt, M., Torn, M., Abiven, S., Dittmar, T., Guggenberger, G., Janssens, I.A., Kleber, M., Kögel-Knabner, I., Lehmann, J., Manning, D.A.C., Nannipieri, P., Rasse, D., Weiner, S., Trumbore, S.E., 2011. Persistence of soil organic matter as an ecosystem property. Nature 478, 49–56. https://doi.org/10.1038/nature10386.

Schöpp, W., Posch, M., Mylona, S., Johansson, M., 2003. Long-term development of acid deposition (1880–2030) in sensitive freshwater regions in Europe. Hydrology and Earth Sciences 7 (4), 436–446. https://doi.org/10.5194/hess-7-436-2003.

Shi, Z., Chow, C.W.K., Fabris, R., Liu, J., Jin, B., 2022. Applications of online UV-Vis spectrophotometer for drinking water quality monitoring and process control: a review. Sensors 22 (8), 2987. https://doi.org/10.3390/s22082987.

Solberg, C.O., 2022. Clarifying the role of ferric iron for Dissolved Natural Organic Matter ultraviolet and visible light absorbance. University of Oslo. MSc thesis.

Svensson, M., Jansson, P.-E., Berggren, K.D., 2008. Modelling soil C sequestration in spruce forest ecosystems along a Swedish transect based on current conditions. Biogeochemistry 89 (1), 95–119. https://doi.org/10.1007/s10533-007-9134-y.

Thrane, J.E., Hessen, D.O., Andersen, T., 2014. The absorption of light in lakes: Negative impact of dissolved organic carbon on primary productivity. Ecosystems 2014 (17), 1040–1052.

Tipping, E., Hurley, M.A., 1988. A model of solid-solution interactions in acid organic soils, based on the complexation properties of humic substances. J. Soil Sci. 39, 505–519. https://doi.org/10.1111/j.1365-2389.1988.tb01235.x.

Tipping, E., Elias, J.L., Keenan, P.O., Helliwell, R.C., Pedentchouk, N., Cooper, R.J., Buckinham, S., Gjessing, E., Ascough, P., Bryant, C.L., Garnett, M.H., 2022. Relationships between riverine and terrestrial dissolved organic carbon: Concentration, radiocarbon signature, specific UV absorbance. Sci. Total Environ. 817. https://doi.org/10.1016/j.scitotenv.2022.153000.

Turner, R.C., Miles, K.E., 1957. The ultraviolet absorption spectra of the ferric ion and its first hydrolysis product in aqueous solutions. Can J Chem 35 (9), 1002–1009.

Vargas Godoy, M.R., Markonis, Y., Rakovec, O., Jenicek, M., Dutta, R., Pradhan, R.K., Beštáková, Z., Kyselý, J., Juras, R., Papalexiou, S.M., Hanel, M., 2024. Water cycle acceleration in Czechia: A water budget approach. Hydrol. Earth Syst. Sci. 28, 1–19. https://doi.org/10.5194/hess-28-1-2024.

Verwey EJW, Overbeek JTG. Theory of stability of lyophobic colloids. Elsevier 1948, 108p. Amsterdam.

Vogt, R.D., Egil, G., Andersen, D.O., Clarke, N., Gadmar, T., Bishop, K., Lundstrøm, U., Starr, M., 2001. Natural Organic Matter in the Nordic countries. Nordtest 156. https://www.nordtest.info/wp/2001/10/29/natural-organic-matter-in-the-nordic-countries-nt-tr-479/.

Vogt RD, Andersen DO, Andersen S, Christophersen N, Mulder J. Streamwater, soil-water chemistry, and water flow paths at Birkenes during a dry-wet hydrological cycle. in the surface water acidification programme (ed B.J. Mason) 149-154 (Cambridge Univ. Press, 1990). ISBN: 0-521-39533-X.

Vogt, R.D., Porcal, P., Hejzlar, J., Paule-Mercado, M.C., Haaland, S., Gundersen, C.B., Orderud, G.I., Eikebrokk, B., 2023. Distinguishing between sources of natural dissolved organic matter (DOM) based on its characteristics. Water 15 (16), 3006. https://doi.org/10.3390/w15163006.

Weishaar, J.L., Aiken, G.R., Bergamaschi, B.A., Fram, M.S., Fujii, R., Mopper, K., 2003. Evaluation of specific ultraviolet absorbance as an indicator of the chemical composition and reactivity of dissolved organic carbon. Environ. Sci. Technol. 37 (20), 4702–4708. https://doi.org/10.1021/es030360x.

Yang, B., Cheng, X., Zhang, Y., Li, W., Wang, J., Guo, H., 2021. Probing the roles of pH and ionic strength on electrostatic binding of tetracycline by dissolved organic matters: re-evaluation of modified fitting model. Environ. Sci. Ecotechnol. 8, 100133 https://doi.org/10.1016/j.ese.2021.100133.

Zahradníček, P., Brázdil, R., Štěpánek, P., Trnka, M., 2021. Reflections of global warming in trends of temperature characteristics in the Czech Republic, 1961–2019. Int. J. Climatol. 41, 1211–1229. https://doi.org/10.1002/joc.6791.

Zaitchik, B.F., Rodell, M., Biasutti, M., Seneviratne, S.I., 2023. Wetting and drying trends under climate change. Nat. Water 1, 502–513. https://doi.org/10.1038/s44221-023-00073-w.

Znachor, P., Nedoma, J., Hejzlar, J., Seďa, J., Kopáček, J., Boukal, D., Mrkvička, T., 2018. Multiple long-term trends and trend reversals dominate environmental conditions in a man-made freshwater reservoir. Sci. Total Environ. 624, 24–33. https://doi.org/10.1016/j.scitotenv.2017.12.061.

Znachor P. Rimov reservoir – Czechia. Site Funding Agency: Czech Science Foundation (GACR). 2022. https://deims.org/ef2ae321-6e94-4170-9616-9a54f529643c.